nzsee
NEW ZEALAND SOCIETY FOR EARTHQUAKE ENGINEERING

Effects of spatial soil variability in 2D ground response models of Wellington

C.R. McGann & B.A. Bradley
Department of Civil and Natural Resources Engineering, University of Canterbury, Christchurch.

S. Jeong
School of Engineering, The University of Waikato, Hamilton.

ABSTRACT

Current analytical techniques for seismic ground response analysis are largely based on 1D wave propagation assumptions, while the growing body of evidence indicates that 1D analysis is only appropriate at a minority of sites. The limitations of 1D analysis come from mechanisms related to how the site is modelled, e.g. wave scattering from small-scale soil heterogeneity cannot be captured, and how the site is defined, e.g. no consideration for basin edge effects or 2D/3D geometry. This paper investigates how consideration for some of these missing factors affects the surficial site amplification for a strong motion recording site in Wellington, New Zealand. Plane strain analyses of the surficial soils and underlying basin materials and geometry are conducted with consideration for the spatial variability of the surficial soils across the model through random variations of an underlying simplified profile. The differences in results between this approach and 1D wave propagation methods are discussed and assessed.

1 INTRODUCTION

Wellington is located at the southern end of the North Island of New Zealand. The geotechnical conditions in central Wellington are quite complex and variable, with the surficial geology shifting from bedrock in the surrounding hills to Pleistocene deposits and Holocene sediments and reclaimed land near the waterfront (Semmens et al., 2010). The Thorndon basin (see Figure 1) extends from the Wellington fault east through the northern part of central Wellington to the harbor. The Wellington fault has dip and rake angles of 80° and 15° (Litchfield et al., 2012), creating both a steep-sided soil basin as well as a deeper bedrock basin formed by the potential horizontal velocity contrast from the more intact and less weathered rock of the western footwall and the relatively more weathered and fractured rock in the eastern hanging wall (Van Dissen and Berryman, 1996).

Surficial ground motion records from strong motion stations in Wellington show clear evidence of both local site effects and basin-edge effects (Holden et al., 2013; Bradley et al., 2018). These basin-edge effects were

particularly evident for sites located in the Thorndon basin during the 2016 Kaikōura earthquake, where shaking in the 1-2 second period range exceeded the 500-year return-period ground motions. A preliminary 2D numerical study by McGann et al. (2019) used plane strain ground response models to demonstrate the clear difference between 1D and 2D ground response analyses for a site in the Thorndon basin. This paper extends upon this previous study to examine the effects of random spatial variation within the soil domain and the ability of such random models to capture the inherent complexity of the Wellington region relative to simplified descriptions.

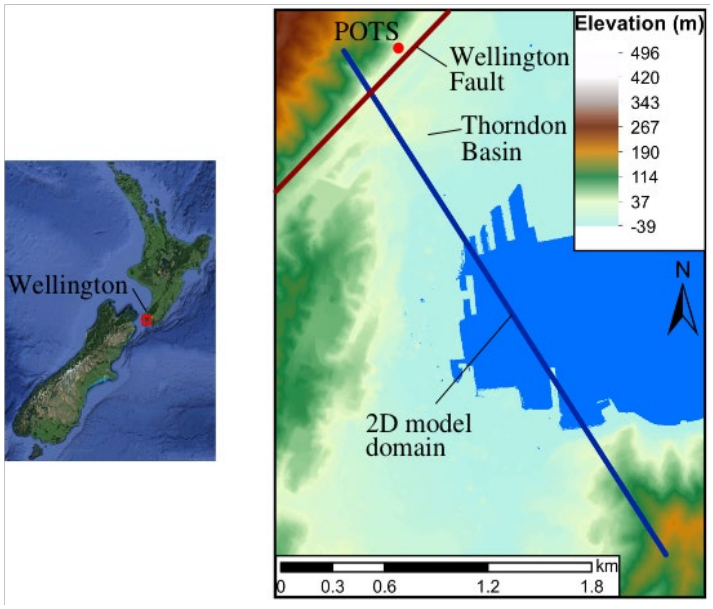

Figure 1: Location, orientation, and extents of 2D model domain across Wellington. Background contours show ground surface elevation.

2 MODEL DEVELOPMENT

Plane strain models of a vertical slice through the Thorndon basin are developed and analysed using the OpenSees finite element analysis platform (McKenna, 2011). All models use the stabilized reduced integration quadrilateral elements of McGann et al. (2012) and consider only linear elastic constitutive response. The general model development is summarized in the following sections, with emphasis on the development of the spatially varying random fields. Further model development details are provided in McGann et al. (2019).

2.1 Basin geometry and material properties

The considered model domain shown in Figure 1 extends from the hills northwest of central Wellington across the Wellington fault, through the Thorndon basin, across the harbor, ending in the southeastern hills. The ground surface is based on digital elevation data and the Semmens et al. (2010) bedrock depth model informs the subsurface boundaries and layers. Bathymetry data are used in offshore regions where the Semmens et al. (2010) model is poorly constrained by measurements.

The elevation layout of the basin model is shown in Figure 2(a), which depicts both the mesh in the domain of interest and the layout of the various subsurface layers considered. For reference, the domain shown in Figure 2(a) is approximately 3.25 km wide and 433 m tall at the horizontal extents. The element size varies throughout the model domain with a smooth transition from an average element size of 2-4 m near the ground surface, to an average size of 15 m at greater depths. These element sizes limit the frequency content that can be transmitted through the model, and a compromise between frequency content and computational

efficiency was sought when developing the mesh. Elements are smaller near interfaces, the ground surface, and the site of interest.

The Wellington fault is clearly evident in Figure 2(a) as the boundary between the two bedrock layers. The rock layers are assigned constant shear wave velocities of 800 m/s in the weathered rock, 1000 m/s in the bedrock on the hanging wall side, and 2000 m/s on the footwall side. These values are assumed based on information provided in Semmens et al. (2010). Consideration for this horizontal impedance contrast across the fault creates a deeper rock basin that was shown to better match recorded motions by McGann et al. (2019). This horizontal velocity contrast is also consistent with the seismic history of the Wellington fault, as findings by Van Dissen and Berryman (1996) indicate that fracturing and secondary faults are likely present on the hanging wall side of the fault, resulting in a reduced stiffness relative to the foot wall side. All rock densities are taken as 2.6 Mg/m^3 after Tenzer et al. (2010).

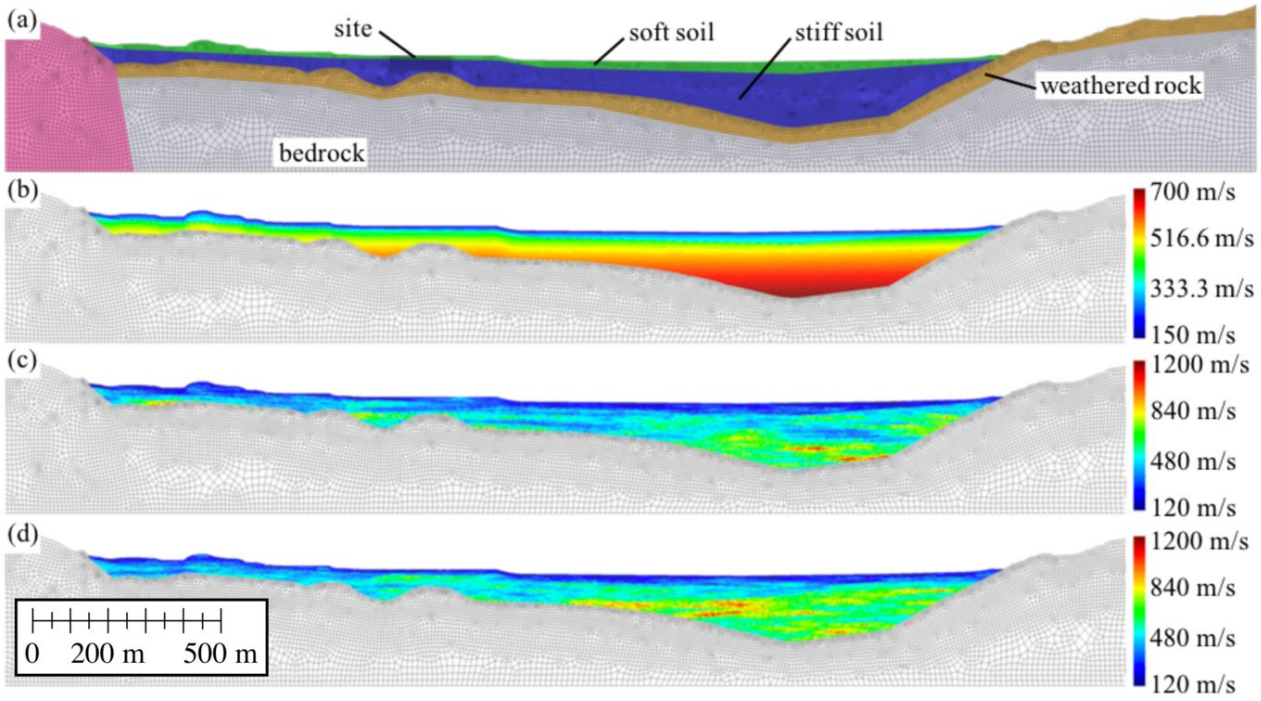

Figure 2: Mesh and shear wave velocity profile summary for 3250 m wide and 433 m high model domain. (a) Mesh and assumed layering; (b) Baseline depth-dependent shear wave velocity distribution in soil domain; (c) and (d) Random anisotropic shear wave velocity realisations.

Figure 2(b) shows the baseline soil shear wave velocity distributions used to inform the development of the random fields. The soil domain is roughly divided into two layers, a layer of softer soils near the surface and a deeper layer of more dense and stiff soils. Simple depth-dependent power law functions are assumed for the shear wave velocities within these soil layers such that $V_s = 160z^{0.25}$ in the soft soils and $190z^{0.25}$ in the stiff soils, where z is the depth below the ground surface. These velocity distributions and the general layer profile assumed in these models are based on available SPT and CPT test data in Wellington city to indicate major layer boundaries, and the surface wave-based shear wave velocity characterization of the central city by Cox and Vantassel (2018). The general values assigned to various soil deposits by Semmens et al. (2010) are also used in developing the simplified shear wave velocity distribution in the model soil domain. The mass densities of the soft and stiff layers are assumed as 1.7 and 1.8 Mg/m^3, respectively. The elastic constitutive model used in these analyses for the rock and soil layers is defined using the shear modulus corresponding to the assigned shear wave velocity and density of each element and an assumed Poisson's ratio of 0.3 for all elements and materials.

2.2 Random field models of soil shear wave velocity

The effects of spatial variability in the near-surface soils are examined by generating spatially-varying random fields for the shear wave velocities within the soft and stiff soil layers. These random fields are computed using an exponential model and the randomization method (e.g., Heße et al., 2014). The simple depth-dependent shear wave velocity profile of Figure 2(a) taken as the mean value for each soil element and a standard deviation of the natural logarithm of V_s is assumed to be 0.2 throughout the soil domain. The horizontal autocorrelation length is set as 80 m and 100 m in the soft and stiff soil layers, respectively. Two isotropy conditions are considered in this study, a fully isotropic condition where the vertical autocorrelation length is the same as the horizontal and an anisotropic condition where the vertical autocorrelation length is one tenth of the horizontal in each soil layer, i.e. the vertical autocorrelation length is 8 m in the soft soil and 10 m in the stiff soil. This anisotropy ratio was selected for initial assessment in this study. Future work will investigate other anisotropy ratios. Ten realizations of the random velocity fields are developed and analysed for both the isotropic and anisotropic conditions. Figures 2(c) and (d) show two examples of the anisotropic random fields developed, highlighting the velocity variability and the effect of the anisotropic variation.

2.3 Boundary and loading conditions

Periodic boundaries are enforced at the horizontal extents of the models, which are extended out past those shown in Figure 2 in an attempt to eliminate boundary effects near the middle. A horizontal input motion is applied at the base of the mesh to account for compliant base conditions after Joyner and Chen (1975). The input ground motion recorded at the POTS strong motion station (see Figure 1) from the 16 August 2013 M_w6.6 Lake Grassmere earthquake is considered in the current study. The POTS station is sited on a rock outcrop, and a deconvolution of this record is the best available approximation for the ground motion within the bedrock below Wellington for the selected ground motion. For simplicity, spatial variability of the incident motion is ignored and the deconvolved POTS motion is assumed across the entire model as a vertically-propagating SH-wave. This treatment of the boundaries and load application is greatly simplified and not entirely appropriate given the velocity contrast across the fault, but it is useful and sufficient for the purposes of this study.

3 EXAMINATION OF RESULTS AT SITE OF INTEREST

An initial assessment of the model results is undertaken at a site of interest located near the approximate centre of the Thorndon basin part of central Wellington. This site is selected to support ongoing analysis of a structure that was instrumented with accelerometers during the Lake Grassmere earthquake. The selected site is located less than 50 m from strong motion recording station and about 0.5 km from the POTS station. The depth to bedrock at this site is approximately 45 m and the structure is sited on approximately 8-10 m of reclamation fill underlain by stiffer soils.

Figures 3 and 4 show the horizontal response spectra and the amplification of the horizontal motion relative to the input POTS motion for the anisotropic and isotropic random field cases, respectively (all horizontal motions are rotated into the plane of the model domain). The results for all ten random realizations are shown in grey and the average response across all ten models is shown in blue. For additional context, several other results are also shown in Figures 3 and 4: the observed response at the nearby strong motion station, the response at the site of interest in a model using the baseline shear wave velocity profile shown in Figure 2(b), and the results of an SH-1D site response analysis using the soil and rock profile directly below the site of interest. As shown in Figure 3, all of the plane strain models compare better to the observed ground response than the 1D analysis, particularly in the 0.8-1.6 second period range where basin-edge effects are evident in the observed results.

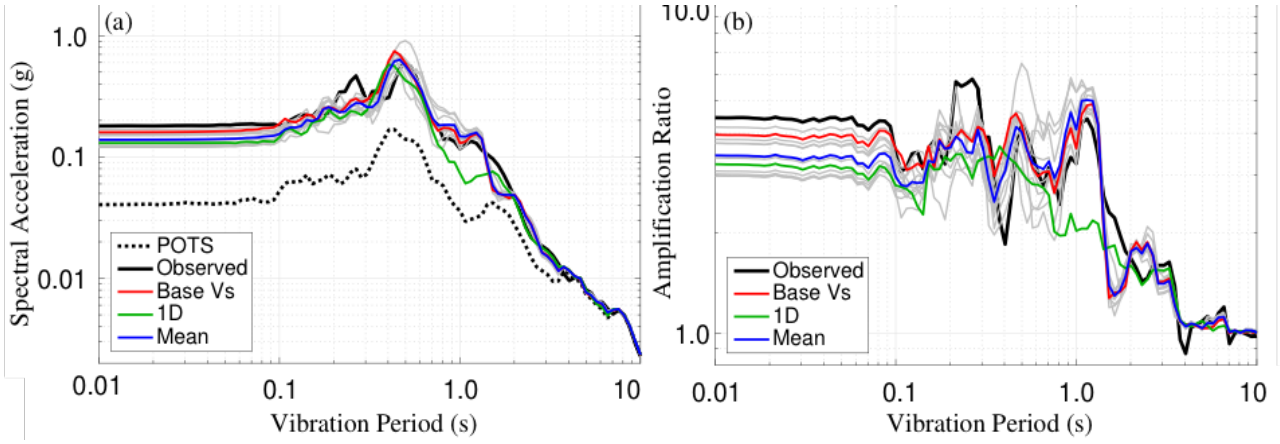

Figure 3: Horizontal results at site of interest for anisotropic cases relative to input POTS motion, observed surface response, model results using baseline Vs profile, and 1D site response analysis. Results of all 10 realizations are shown in grey, and the mean of these 10 models is shown in blue. (a) Response spectra; (b) Spectral amplification of POTS record.

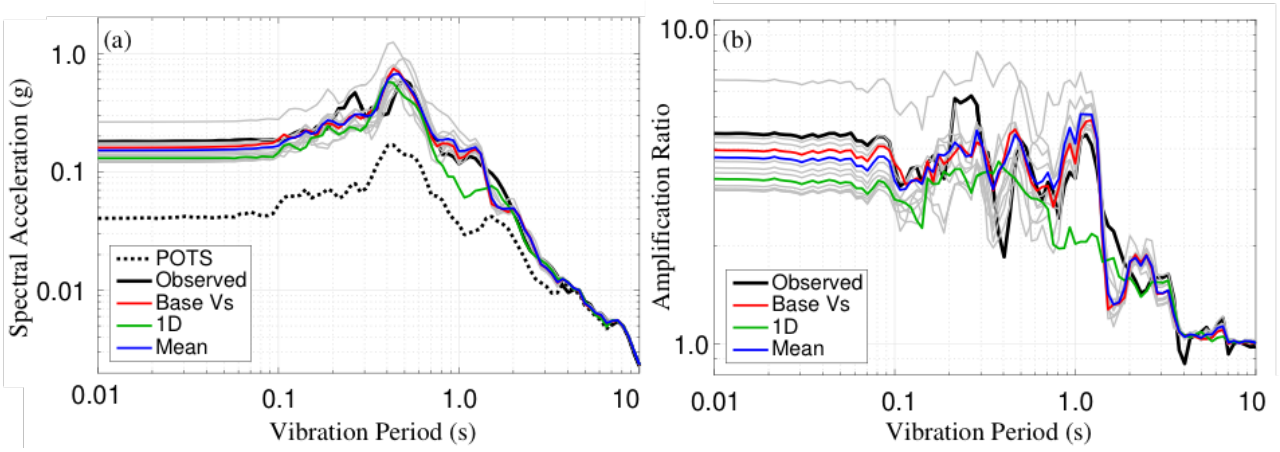

Figure 4: Horizontal results at site of interest for isotropic cases relative to input POTS motion, observed surface response, model results using baseline Vs profile, and 1D site response analysis. Results of all 10 realizations are shown in grey, and the mean of these 10 models is shown in blue. (a) Response spectra; (b) Spectral amplification of POTS record

Figures 3 and 4 also indicate that while there are certainly variations between the results of the ten distinct random velocity fields, the baseline model results are not significantly different from the average response of the ten realizations for either the anisotropic or isotropic random field models (beyond the clear difference at low periods). Also, while the anisotropic cases appear to be superior to the isotropic cases, this is largely due to a single outlier case in the isotropic realizations where there appears to be nearly continuous horizontal zones of higher shear wave velocities throughout the stiff soil layer, essentially creating a large horizontal impedance boundary within this layer whereas the other realizations tend to have intermittent zones of lower velocities breaking up the higher velocity zones and creating vertical and inclined impedance boundaries. These observations are likely functions of the relatively small number of cases currently considered.

For the anisotropic cases, an examination of the individual amplification ratios shown in Figure 3(b) indicates that several of the random velocity cases match the observed amplification significantly better than the average over certain period ranges, however, none of the 10 anisotropic cases matches the observations well across all periods. This offers more evidence that more realizations are likely necessary to get a comprehensive assessment of the site, however, the results from the ten anisotropic cases here would likely be sufficient for design purposes as they tend to envelope the true site response.

Figure 5 shows the vertical spectral response at the site of interest for the anisotropic cases, again with comparisons to the observed response at the nearby strong motion station and the corresponding response using the baseline shear wave velocity distribution of Figure 2(b). Because there is no vertical input motion applied to the 2D models, the vertical acceleration recorded at the POTS station is added to the model vertical accelerations in Figure 5(a) to aid in comparisons to the observed surface response. The recorded vertical acceleration was not applied in the model, only to aid in interpreting the results in this plot - the simulated vertical response spectra are also shown in Figure 5(b) without this addition. As shown in Figure 5(a), none of the models compare well to the observed response. This discrepancy is expected, as the observed vertical response consists of body and surface waves acting in all orientations, not just in the plane selected here. The average response from the random field models is relatively similar to the results of the baseline model, however, the vertical spectral accelerations of the random cases tend to be greater than or equal to the baseline model at nearly all periods.

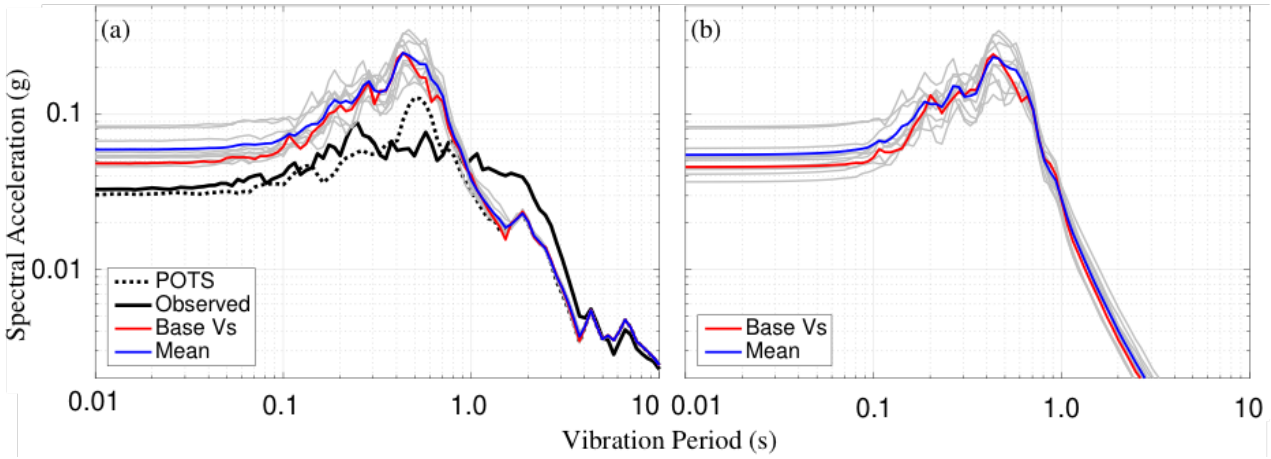

Figure 5: Vertical results at site of interest compared to input POTS motion, observed surface response, and model results using baseline Vs profile. Results of all 10 realizations are shown in grey, and the mean of these 10 models is shown in blue. (a) Response spectra for sum of POTS vertical acceleration with simulated vertical motions; (b) Vertical response spectra of simulated surficial motions alone.

Due to the use of a solely horizontal input motion in the plane strain models, the simulated vertical response at the site of interest can only be caused by body waves, non-vertically incident shear waves, and surface waves generated by waves propagating through the models. The random field model results do not display any significantly different trends relative to the baseline model in terms of intensity of waves in different period ranges, but the scatter in the results in Figures 4(a) and (b) indicates that the composition of the velocity structure within each random field realization influences the amplitude and frequency content of the basin-generated surface waves (and non-vertically incident shear waves) at the site of interest within the models

4 CONCLUSIONS AND FUTURE WORK

Plane strain models through the Thorndon basin in Wellington, New Zealand were developed and analyzed to assess the influence of spatially-varying random shear wave velocity distributions throughout the near-surface basin soils at a reference site in central Wellington. The random fields were generated using an exponential model, and two isotropy conditions were considered, a fully isotropic condition and an anisotropic condition in which the vertical autocorrelation length was one tenth of the horizontal autocorrelation length. Ten random realizations for each isotropy condition were analyzed and the results were compared to observations at a strong motion station adjacent to the reference site in terms of horizontal and vertical response spectra and spectral amplification relative to a reference rock site.

Comparisons of the horizontal and vertical accelerations at the reference site in the random field models to the observed values as well as simplified 1D and 2D numerical models showed that the random field realizations tend to envelope the observed response, with the same deficiencies as the baseline plane strain models with a simplified depth-dependent soil shear wave velocity distribution. No significant differences were observed between the results of the isotropic and anisotropic random field models, though this is likely a function of the relatively small sample size of realizations considered in this work and the consideration for only a single anisotropy condition at this stage in the research. While none of the random field models matched the observations at all periods, individual realizations matched the observed spectral accelerations better than the simplified baseline model over certain period ranges.

Even with the somewhat limited database of cases currently considered, the ability of the random field models to aid in design decision making for future prediction analysis is highlighted by these preliminary results. Generating the random fields and running the additional analyses is not computationally burdensome, and this computational cost is worth the investment given the potential for better understanding made available by the additional cases. In terms of future work, analyses of more realizations and more combinations of random field model parameters, including variations in the standard deviation of the velocity field, the horizontal autocorrelation length, and the associated vertical autocorrelation length (i.e. anisotropy condition) are currently underway. Future studies will also aim to investigate linking the random field model parameters to the conditions in Wellington, and introducing corresponding random velocity fields into the underlying rock layers. This work is being undertaken with the intention of both assessing the effects and relative importance of the various model choices on the simulation results, and further assessing the effects of the random soil shear wave velocities on the 2D site response in the Thorndon basin and how the results of these models compare to the observations made in recent moderate to large earthquakes.

5 ACKNOWLEDGEMENTS

Elevation and bathymetry data were sourced from the LINZ Data Service (https://data.linz.govt.nz) and licensed by the Wellington Regional Council for re-use under the Creative Commons Attribution 4.0 International license. All seismograms were obtained from the New Zealand Strong Motion Database (Van Houtte et al., 2017). The random fields were generated using GeoStat-Framework/GSTools 1.01 (https://pypi.org/project/gstools/) under the GNU General Public License v3.0. This work was supported by QuakeCoRE, a New Zealand Tertiary Commission-funded Centre. This is QuakeCoRE publication number 0379.

REFERENCES

Afshari, K. & Stewart, J.P. 2015. Effectiveness of 1D ground response analyses at predicting site response at California vertical array sites. *Proc., CSMIP Seminar on Utilization of Strong Motion Data*, Sacramento, CA.

Bradley, B.A., Wotherspoon, L.M., Kaiser, A.E., Cox, B.R., & Jeong, S. 2018. Influence of site effects on observed ground motions in the Wellington region from the Mw7.8 Kaikōura, New Zealand, earthquake. *Bulletin of the Seismological Society of America*, Vol 108(3B) 1722-1735.

Cox, B.R. & Vantassel, J. 2018. *Dynamic Characterization of Wellington, New Zealand*. DesignSafe-CI [publisher], Dataset, doi: 10.17603/DS24M6J

Heße, F., Prykhodko, V. Schülter, S., & Attinger, S. 2014. Generating random fields with a truncated power-law variogram: A comparison of several numerical methods. *Environmental Modeling & Software*, Vol 55 32-48.

Holden, C., Kaiser, A., Van Dissen, R., & Jury, R. 2013. Sources, ground motion and structural response characteristics in Wellington of the 2013 Cook Strait earthquakes. *Bulletin of the New Zealand Society for Earthquake Engineering*, Vol 46(4) 188-195.

Joyner, W.B. & Chen, A.T.F. 1975. Calculation of nonlinear ground response in earthquakes. *Bulletin of the Seismological Society of America*, Vol 65(5) 1315-1336.

Kaklamanos, J. & Bradley B.A. 2013. Critical parameters affecting bias and variability in site-response analyses using KiK-net downhole array data. *Bulletin of the Seismological Society of America*, Vol 103 1733-1749.

Litchfield, N.J., Van Dissen, R., Sutherland, R., Barnes, P.M., Cox, S.C., Norris, R., Beavan, R.J., Langridge, R., Vilamor, P., Berryman, K., Stirling, M., Nicol, A., Nodder, S., Larmarche, G., Barrell, D.J.A., Pettinga, J.R., Little, T., Pondard, N., Moutjoy, J., & Clark, K. 2012. *A Model of Active Faulting in New Zealand: Fault Zone Parameter Descriptions*. GNS Science Report 2012/19. GNS, Lower Hutt, New Zealand.

McGann, C.R., Arduino, P., & Mackenzie-Helnwein, P. 2012 Stabilized single-point 4-node quadrilateral element for dynamic analysis of fluid saturated porous media. *Acta Geotechnica*, Vol 7(4) 297-311.

McGann, C.R., de la Torre, C.A., & Bradley, B.A. 2019. Plane strain modeling of basin-edge effects: exploratory study in Wellington, New Zealand. *Proc., 7th International Conference on Earthquake Geotechnical Engineering (7ICEGE)*, June 17-20, Rome, Italy.

McKenna, F. 2011. OpenSees: A framework for earthquake engineering simulation. *Computing in Science and Engineering*, Vol 13(4) 58-66.

Semmens, S. Perrin, N.D., & Dellow, G.D. 2010. *It's Our Fault – Geological and Geotechnical Characterisation of the Wellington Central Business District*. GNS Science Consultancy Report 2010/176, GNS, Lower Hutt, New Zealand.

Tenzer, R., Sirguey, P., Rattenbury, M., & Nicolson, J. 2010. A digital rock density map of New Zealand. *Computers & Geosciences*, Vol 37(8) 1181-1191.

Thompson, E.M., Baise, L.G., Kayen, R.E., & Guzina, B.B. 2009. Impediments to predicting site response: seismic property estimation and modeling simplifications. *Bulletin of the Seismological Society of America*, Vol 99(5) 2927-2949.

Thompson, E.M., Baise, L.G., Tanaka, Y., & Kayen, R.E. 2012. A taxonomy of site response complexity. *Soil Dynamics and Earthquake Engineering*, Vol 41 32-43.

Van Dissen, R.J. & Berryman, K.R. 1996. Surface rupture earthquakes over the last 1000 years in the Wellington region, New Zealand, and implications for ground shaking hazard. *Journal of Geophysical Research*, Vol 101(B3) 5999-6019.

Van Houtte, C., Bannister, S., Holden, C., Bourguignon, S., & McVerry, G. 2017. The New Zealand Strong Motion Database. *Bulletin of the New Zealand Society for Earthquake Engineering*, Vol 50(1) 1-20.